Journal of Alloys and Compounds 506 (2010) 950–955

Contents lists available at ScienceDirect

Journal of Alloys and Compounds

journal homepage: www.elsevier.com/locate/jallcom

Electronic properties and europium ion photoluminescence behaviors in Sr_2CeO_4 phosphor

Jie Li[a,b], Li Wang[a], Hefeng Zhou[a], Xuguang Liu[a,c], Bingshe Xu[a,d,*]

[a] Key Laboratory of Interface Science and Engineering in Advanced Materials (Taiyuan University of Technology), Ministry of Education, Taiyuan, 030024, PR China
[b] College of Materials Science and Engineering, North University of China, Taiyuan, 030051, PR China
[c] College of Chemistry and Chemical Engineering, Taiyuan University of Technology, Taiyuan, 030024, PR China
[d] College of Materials Science and Engineering, Taiyuan University of Technology, Taiyuan, 030024, PR China

ARTICLE INFO

Article history:
Received 20 February 2010
Received in revised form 11 July 2010
Accepted 12 July 2010
Available online 23 July 2010

Keywords:
Electronic structures
Photoluminescence
Sr_2CeO_4 phosphor
Energy transfer

ABSTRACT

Sr_2CeO_4, pure and doped with Eu^{3+} ions of different concentrations, were synthesized by polyacrylamide gel method. First principles were applied to calculate the electronic structures and band gap of Sr_2CeO_4. The results show that a broad emission band originating from Sr_2CeO_4 host and Eu^{3+} emission lines in blue, green, and red regions coexist. The increase in Eu^{3+} concentration results in the luminescence intensity redistribution between the Sr_2CeO_4 host and the doping ion. The energy transfer model clarifies the possible mechanisms of energy transfer from Sr_2CeO_4 host to Eu^{3+} in Sr_2CeO_4:Eu^{3+} phosphor.
© 2010 Elsevier B.V. All rights reserved.

1. Introduction

Oxide-based phosphors were widely utilized in various opto-electronic and displaying devices due to their high thermal stability, chemical stability and excellent optical properties [1–4]. An unusual blue phosphor Sr_2CeO_4 was first prepared using the combinatorial techniques by Danielson et al. in 1998 [5]. Since then, many advanced synthesis techniques such as Pechini's method [6], spray pyrolysis [7], emulsion liquid membrane system [8], ethylenediaminetetraacetic acid (EDTA)-complexing process [9], microwave-assisted solvothermal process [10] have been developed to prepare the Sr_2CeO_4 phosphor because of its efficient luminescence under ultraviolet, cathode ray and X-ray excitation [11,12].

The broad excitation spectrum in the 200–400 nm UV range indicates the feasibility of Sr_2CeO_4 phosphor to be utilized in ultraviolet light emitting diodes (UV-LEDs) [13,14]. However, when Sr_2CeO_4 phosphors are used for UV-LEDs, they cannot produce strong emission. In order to improve illumination efficiency of Sr_2CeO_4, tin (IV) ions were used to replace cerium ions in the host in attempt to increase the excitation intensity in the UV range by Hsu et al. [15].

Moreover, owing to its broad emission band, Sr_2CeO_4 can be used as the matrix material, which may provide a new method to search for future attracting luminescence hybrids under ultraviolet excitation. Until now, the Sr_2CeO_4 lattice is the only host-lattice in which charge-transfer (CT) luminescence of Ce^{4+} has been observed at room temperature [16]. Sr_2CeO_4 crystals doped with rare-earth elements were studied earlier [17–20]. According to the literatures, the luminescence properties of rare-earth doped Sr_2CeO_4 were affected by energy transfer from the triplet excited state of the metal-to-ligand-charge-transfer (MLCT) state for Sr_2CeO_4 to the rare-earth ions. However, the treatment of the obtained experimental data has been contradictory and does not permit any conclusion about the mechanisms of the energy transfer from the crystal host to the doping ions. Nag and Narayanan Kutty [21] claimed that after excitation in CeO_6 groups, non-radiative energy transfer took place from the LS band to the CT states of Eu^{3+} or Sm^{3+}. Hirari and Kawamura [22] suggested that this process was a direct energy transfer from the triplet excited state of the metal-to-ligand-charge-transfer (MLCT) state to the intra-4f excited state of Eu^{3+} ion. Further research by Viagin et al. revealed the Förster non-radiative energy transfer under the energy migration condition from Sr_2CeO_4 crystal host to doping europium ions [23].

Considering the above situation, in this paper, we prepared pure and europium ions doped Sr_2CeO_4 by polymer-network gel method. The method is a wet chemical process that is simple, fast, cheap, reproducible and easily scaled up to obtain a wide variety of fine powders at relatively low temperatures [24]. The electronic

* Corresponding author. Tel.: +86 0351 6014852; fax: +86 0351 6010311.
E-mail address: xubs@tyut.edu.cn (B. Xu).

0925-8388/$ – see front matter © 2010 Elsevier B.V. All rights reserved.
doi:10.1016/j.jallcom.2010.07.126

structures and band gap of Sr_2CeO_4 were calculated by using the CASTEP code with density-functional theory (DFT) method and the results were compared with the experimental data. Our goal in this work is to provide a complete characterization of the photoluminescence (PL) properties and clarify the possible mechanisms of energy transfer in Sr_2CeO_4 and Sr_2CeO_4:Eu phosphors.

2. Experimental methods and computational details

Sr_2CeO_4 crystals, pure and doped with Eu ions, were synthesized by polyacrylamide gel method. The dopant concentration in Sr_2CeO_4:Eu varied within 1–5 mol% range. The procedure was as follows: The stoichiometric amounts of $Sr(NO_3)_2$ and $Ce(NO_3)_3{\cdot}6H_2O$ (A.R.) were dissolved in distilled water and mixed under stirring. Subsequently, acrylamide and N, N′-methylene bisacrylamide monomers in a molar ratio of 22:1 were added. The mixture was maintained at 80–90 °C. Ammonium persulfate was added as initiator to the premixed solution in 10% mass-to-volume ratio. A rapid polymerization was observed, forming a white polymeric gel without any precipitation, followed by homogenization and drying in a ceramic mortar at 110 °C for 18 h. Different samples were obtained after subsequent thermal treatment at 1000 °C for 4 h in air with a heating rate of 4 °C/min. The same synthetic procedure was used for the synthesis of Sr_2CeO_4:xEu^{3+} (x = 1, 3 and 5 mol%).

To identify the crystal phase, X-ray diffraction (XRD) analysis was carried out with a powder diffractometer (Rigaku-D/max 2500), using Cu Kα radiation. The microstructures of the samples were studied using a scanning electron microscope (SEM) (JEOL JSM-6700F). The UV–vis absorption and diffusive reflection spectra of the phosphors in solid state were obtained at a Cary 300 spectrophotometer. The photoluminescence (PL) emission spectra were measured at an F-4500 FL spectrophotometer. The luminescence decay curves were recorded from Edinburgh Analytical Instruments F900 by the time-correlated single-photon counting method. All the spectra were recorded at room temperature.

All the calculations in the present work were based on the generalized gradient approximation (GGA) of the DFT theory. CASTEP [25–27] used in the present work was on the basis of plane waves and pseudopotentials. The lattice optimization for the Sr_2CeO_4 was performed by using CASTEP code. The considered valence electrons for Sr, Ce and O were $4s^24p^65s^2$, $4f^15s^25p^65d^16s^2$ and $2s^22p^4$, respectively. A kinetic energy cut-off of 370 eV was used throughout the calculation. All other calculations were performed on the basis of optimized lattice structure.

3. Results and discussion

3.1. Crystal structure and morphology of pure and Eu^{3+} doped Sr_2CeO_4

The crystal structure of Sr_2CeO_4 is shown in Fig. 1a. The compound possesses one-dimensional chain structure of edge-sharing CeO_6 octahedron. There are two molecules per unit cell. Each cerium atom is coordinated by six oxygen atoms. These octahedrons present two trans-terminal Ce–O1 bonds perpendicular to the plane defined by four equatorial O2 atoms, while the Ce–O1 bonds are about 0.1 Å shorter than the Ce–O2 bonds [16].

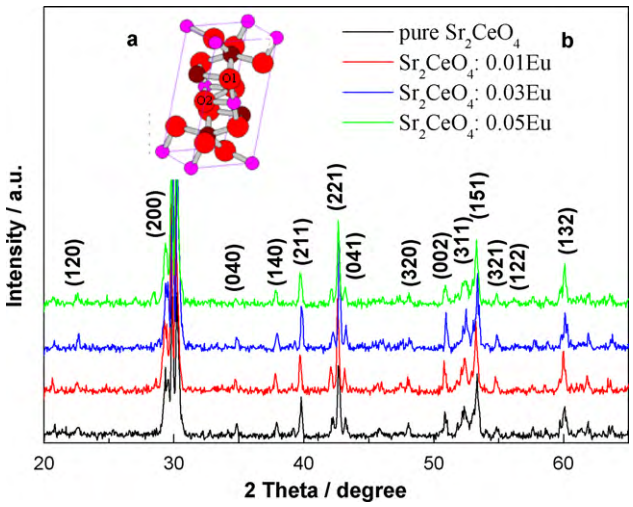

Fig. 1. The crystal structure of Sr_2CeO_4 (a) and the X-ray powder diffraction patterns of pure and Eu^{3+} doped Sr_2CeO_4 (b).

All the prepared Sr_2CeO_4:Eu samples were characterized to be single phase Sr_2CeO_4 of orthorhombic structure with the space group of Pbam (No. 55). The typical XRD patterns of powder samples are shown in Fig. 1b, and all the diffraction peaks were well indexed on the basis of JCPDS No. 50-0115. No other phase was observed in the XRD spectra, indicating that the as-prepared phosphors are single phase and well crystallized. The SEM images of pure and Eu^{3+} doped Sr_2CeO_4 in Fig. 2 clearly show good dispersion and small particle size of the samples. Therefore, the above results demonstrate the potential of polymer-gel process in synthesizing fine powders at relatively low temperatures.

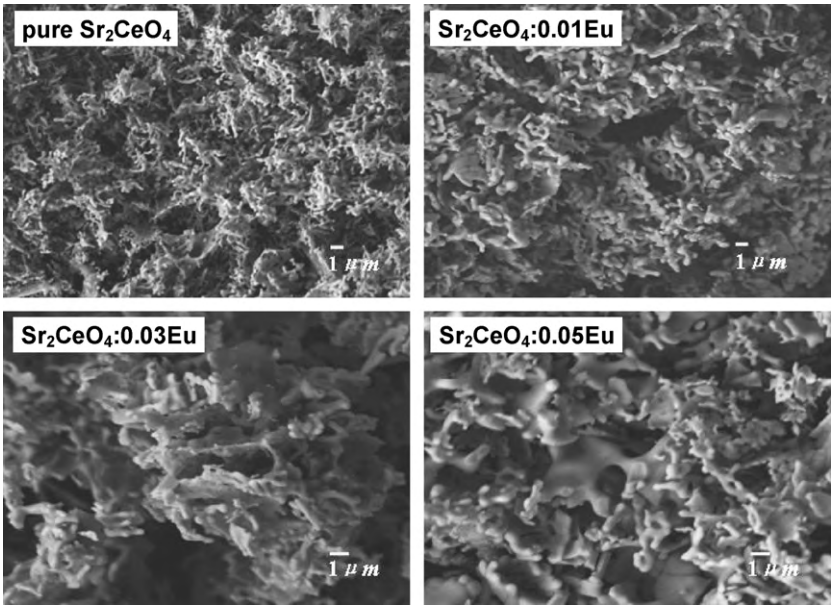

Fig. 2. The SEM images of pure and Eu^{3+} doped Sr_2CeO_4.

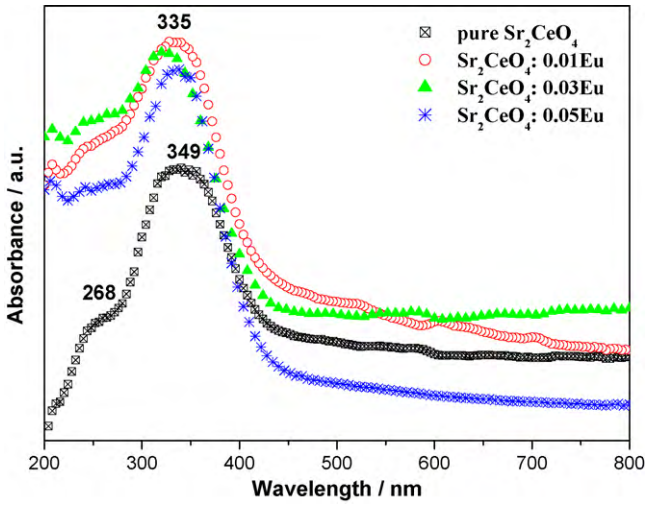

Fig. 3. UV–vis absorption spectra of pure and Eu^{3+} doped Sr_2CeO_4.

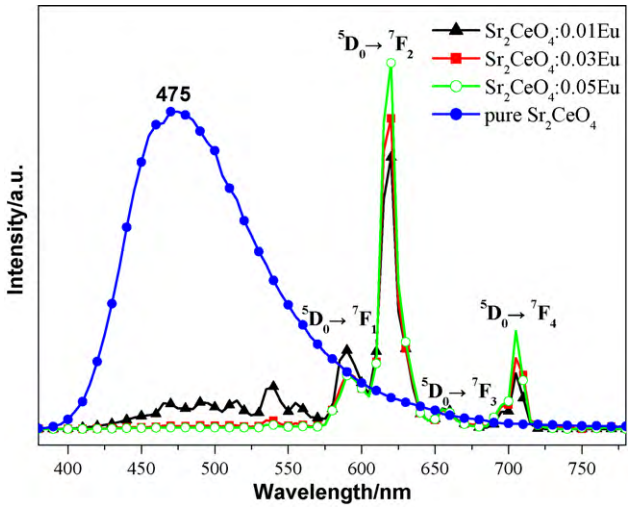

Fig. 5. PL spectra of pure and Eu^{3+} doped Sr_2CeO_4 (λ_{ex} = 349 nm).

3.2. PL behaviors of pure and Eu^{3+} doped Sr_2CeO_4

Fig. 3 shows the UV–vis absorption spectra of pure and Eu^{3+} doped Sr_2CeO_4 phosphor powders. There is no absorption between 450 and 800 nm, indicating the high transparency of the samples in the visible region. The UV–vis absorption spectrum of pure Sr_2CeO_4 is composed of two absorption peaks centering at around 268 nm (4.63 eV) and 349 nm (3.55 eV). For Eu^{3+} doped Sr_2CeO_4, a strong absorption band with maximum value at about 335 nm is observed. In many compounds, the Eu^{3+}–O^{2-} charge-transfer band is generally located at 220–350 nm [17,18]. Therefore, the broad band peaked at 335 nm was ascribed to the overlap of charge-transfer (CT) bands from oxygen to europium (Eu^{3+}–O^{2-}) and the Sr_2CeO_4 host band (Ce^{4+}–O^{2-}). The band gap was determined by measuring the UV–vis diffusive reflection spectra of samples (see Fig. 4). For pure and three Eu^{3+}-doped samples, the band gap values were 2.73 eV (454 nm), 2.75 eV (451 nm), 2.77 eV (448 nm) and 2.86 eV (433 nm), respectively.

The PL spectrum of Sr_2CeO_4 was characterized by a broad band ranging from 390 to 650 nm with a peak position at 475 nm (Fig. 5), which was ascribed to the CT transition of Ce^{4+}–O^{2-} [16]. Actually, the PL spectra for the Sr_2CeO_4:Eu varied considerably with the concentration of Eu^{3+}, as shown in Fig. 5. The PL spectra of Sr_2CeO_4:xEu^{3+} (x = 1, 3 and 5 mol%) consists of the characteristic lines of Eu^{3+} corresponding to transitions from the exited $^5D_0$ level: $^5D_0 \rightarrow {}^7F_1$, $^5D_0 \rightarrow {}^7F_2$, $^5D_0 \rightarrow {}^7F_3$, and $^5D_0 \rightarrow {}^7F_4$ located at 590, 619, 655, and 704 nm, respectively. The red emission intensity of the transition $^5D_0 \rightarrow {}^7F_2$ was the strongest, indicating no inversion symmetry at the site of the rare-earth ion Eu^{3+}. As is well known, if Eu^{3+} occupies a site in the crystal lattice with inversion symmetry, the magnetic-dipole transitions $^5D_0 \rightarrow {}^7F_1$ of Eu^{3+} dominate; if there is no inversion symmetry at the site of Eu^{3+}, the main emission is the electric-dipole transition $^5D_0 \rightarrow {}^7F_2$ [20]. Furthermore, the red emission intensity increased with increasing doping concentration from 1 to 5 mol%. The increase in the dopant concentration resulted in the luminescence intensity redistribution between the host and the dopant. When Eu^{3+}concentration was 1 mol%, the broad emission band originating from Sr_2CeO_4 host itself and the Eu^{3+} emission lines in the blue, green, and red regions coexisted. At higher Eu^{3+} concentration (x = 3 mol%), apart from the prominent line emission from Eu^{3+} ions, a weak broad emission originating from host was also observed, which indicates that the energy transfer probability is slightly below unity. It can also be seen that the host luminescence was totally quenched at 5 mol% of doping europium ions (see Fig. 5). Besides this, for the luminescence of Sr_2CeO_4:Eu, emissions were observed not only from the lowest excited $^5D_0$ level of Eu^{3+} but also from higher energy levels of Eu^{3+} with a weaker intensity. As shown in Fig. 5, the PL spectra of Sr_2CeO_4:Eu^{3+} phosphors also involved the transition emissions from the higher energy levels ($^5D_1$ and $^5D_2$). The presence of emission lines from higher excited states of Eu^{3+} was attributed to the low vibration energy of $CeO_4{}^{4-}$ groups. Multiphonon relaxation by $CeO_4{}^{4-}$ is not able to bridge the gaps between the higher energy levels and the $^5D_0$ level of Eu^{3+} completely, resulting in weak emissions from these levels [20]. Fig. 6 illustrates the CIE chromaticity diagram for the emissions of pure and Eu^{3+} doped Sr_2CeO_4. The emission varied from blue-white light to red-white light and then to red light with increasing doping concentration from 0 to 5 mol%. Therefore, the most immediate applications for Sr_2CeO_4:Eu phosphors are likely to be as multicolor-emitting fluorescence powder.

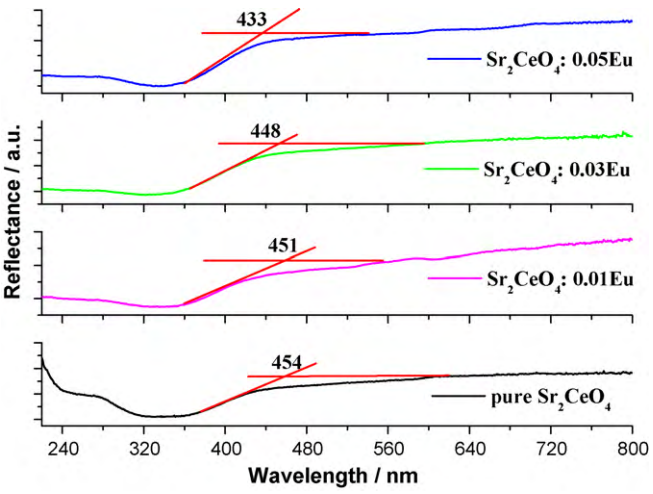

Fig. 4. UV–vis diffusive reflection spectra of pure and Eu^{3+} doped Sr_2CeO_4.

The host luminescence decay was studied at the dopant concentration variation to ascertain the mechanism of crystal host luminescence quenching. The luminescence decay curves are presented in Fig. 7. It is found that after Eu^{3+} doping the lifetime of luminescence from Sr_2CeO_4 host itself at room temperature decreased. The increase in doping ion concentration caused a change in the pattern of the host luminescence decay curves, which is the evidence of the non-radiative energy transfer to the doping

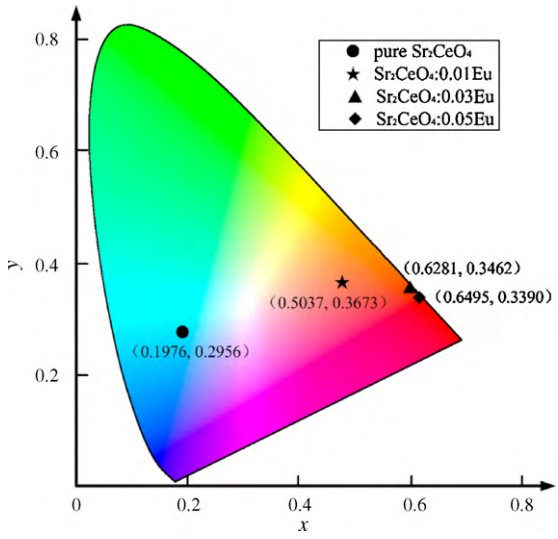

Fig. 6. CIE chromaticity diagram of pure and Eu^{3+} doped Sr_2CeO_4.

ion. Thus, the crystal host is a donor of energy and the doping ion is an acceptor of energy.

3.3. Electronic properties and energy transfer models of pure and Eu^{3+} doped Sr_2CeO_4

It is known that the UV–vis absorption spectrum of Sr_2CeO_4 is attributed to an electron transfer process. This transfer process can occur in two ways: one is a low spin singlet excited state (LS) without a change in spin orientation (a spin-allowed transition, $\Delta S = 0$); the other is a high spin triplet excited state (HS) with a change in spin orientation (a spin-forbidden transition, $\Delta S = 1$) [19]. In order to investigate the energy level distribution of Sr_2CeO_4, the emission spectra of the pure Sr_2CeO_4 phase were deconvoluted. Fig. 8 shows the deconvoluted emission spectrum of Sr_2CeO_4 phosphors. Two emission peaks attributed to two metal-to-ligand-charge-transfer states were observed. This phenomenon is considered to take place because of two different Ce–O bond lengths in CeO_6 octahedra. These two types of Ce–O bond contribute to two different emission maxima, as shown in Fig. 8. The charge-transfer transition processes in two types of Ce–O bond are different in energy. The energy levels of terminal and equatorial metal-to-ligand excited

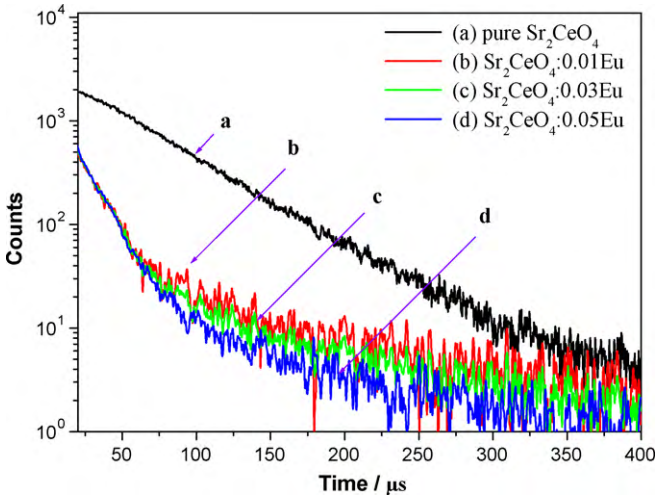

Fig. 7. The luminescence decay curves of pure and Eu^{3+} doped Sr_2CeO_4 at temperature $T = 298$ K ($\lambda_{exc} = 349$ nm, $\lambda_{em} = 475$ nm).

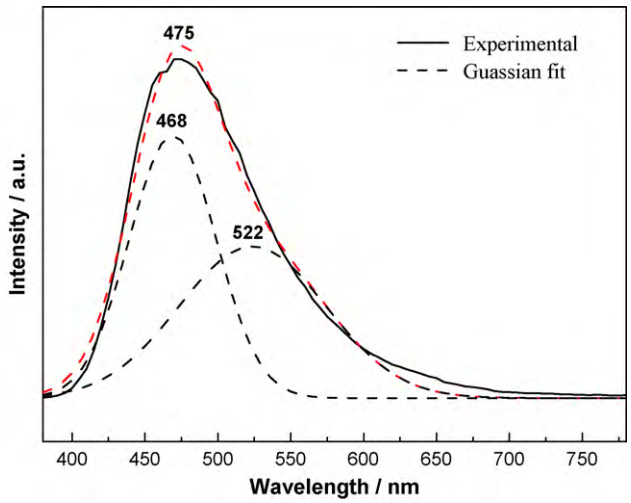

Fig. 8. Deconvoluted PL emission spectrum of Sr_2CeO_4.

states were defined to be 2.65 (468 nm) and 2.38 eV (522 nm) above the ground state, respectively.

Further information was partly collected from the calculated band structure and the electron density of states (DOS) and partial electron density of states (PDOS) of Sr_2CeO_4. Fig. 9 exhibits the direct GGA band gap energy (E_g) of 2.64 eV at G, and the indirect E_g values of 2.68, 2.69, 2.65, 2.63, 2.30, 2.39 and 2.50 eV at Z, T, Y, S, X, U and R, respectively. The theoretical result of E_g, which is 2.64 eV, agrees well with the experiment. The calculated DOS and PDOS of Sr_2CeO_4 in Fig. 10 convey the obvious information that the valence band (VB) is mainly of O 2p orbital and the conduction band (CB) is mainly of Ce 4f orbital in character. Based on the above findings, a qualitative energy level diagram of Sr_2CeO_4 was proposed and the obtained results are illustrated in Fig. 11a. Once an electron is excited from VB to CB, the excited electron rapidly relaxes to the Ce 4f state, followed by transferring to two MLCT states (i.e. $(MLCT)_{terminal}$ and $(MLCT)_{eqatorial}$). When the excited electron is transferred from two MLCT states to VB, two emission peaks appear in the deconvoluted emission spectrum since there is a difference

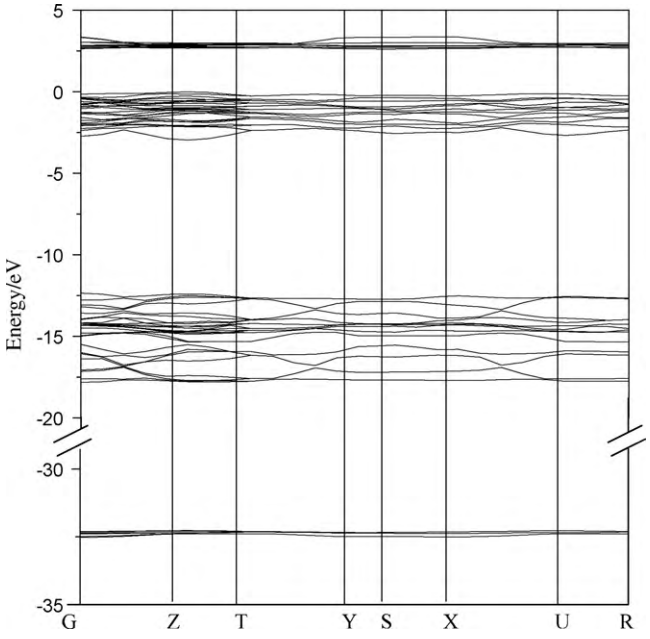

Fig. 9. Calculated band structure of Sr_2CeO_4.

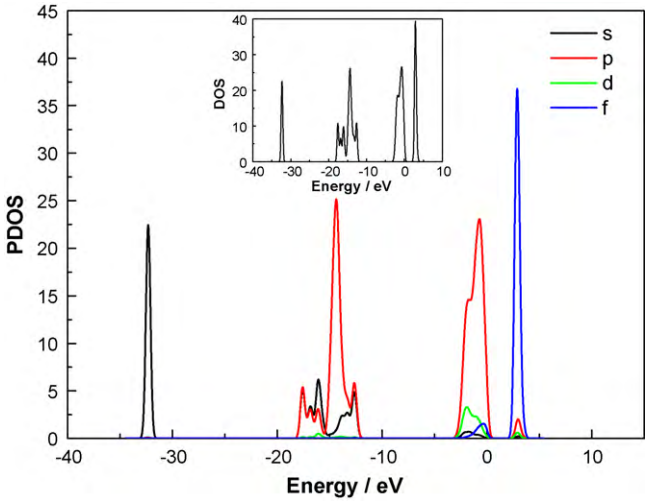

Fig. 10. DOS and PDOS plots of Sr_2CeO_4.

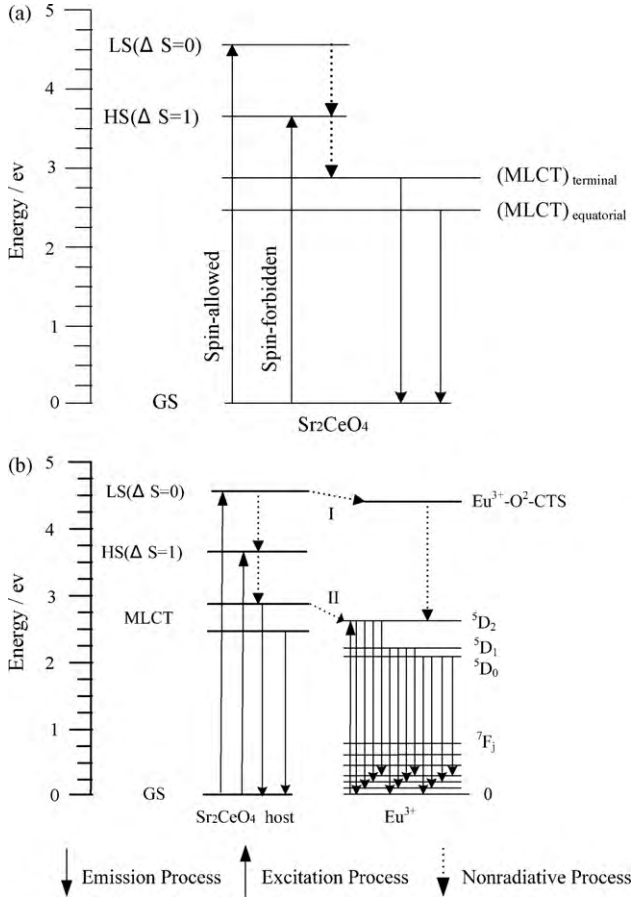

Fig. 11. Energy transfer models of Sr_2CeO_4 (a) and Sr_2CeO_4:Eu (b).

between these two MLCT states. The above behavior explains the wide emission peak of Sr_2CeO_4.

In Sr_2CeO_4:Eu^{3+}phosphor, energy transfer from host to activator Eu^{3+} ions has been reported [17,18]. Eu^{3+}–O^{2-} CT band in Sr_2CeO_4:Eu^{3+} phosphor lies around 4.43 eV. This Eu^{3+}–O^{2-} CT band is very close to the LS band of host (4.63 eV) from which non-radiative energy transfer can easily take place to the former energy levels. Additionally, the HS band of host, which lies at 3.55 eV, causes either emission from MLCT levels or excitation to Eu^{3+} excited levels through non-radiative process. The energy of MLCT level is very close to $^5D_2$ higher excited state of Eu^{3+} ions. This provides another possibility of energy transfer from host to Eu^{3+}ions. Fig. 11b shows a schematic illustration of the above energy transfer process from Sr_2CeO_4 host to Eu^{3+}, where (I) and (II) represent the process from the LS band to CT states of Eu^{3+}–O^{2-} and from the triplet excited state of the MLCT state to the intra-4f excited state of the Eu^{3+} ions, respectively. For Sr_2CeO_4:Eu^{3+} phosphor, with low Eu^{3+} doping concentration, both the process (I) and (II) occur. Thus, emissions from host and $^5D_i \rightarrow {}^7F_j$ (i = 1, 2, j = 0, 1, 2, 3) transition of activator Eu^{3+} are observed at the same. For Sr_2CeO_4:Eu^{3+} phosphor, the higher the Eu^{3+} doping concentration is, the stronger the CT of Eu^{3+}–O^{2-} becomes. When the doping concentration is higher, the process (I) dominates. In other words, the energy absorbed by host transfers from the LS band to CT states of Eu^{3+}–O^{2-}, and then, emission takes place from ^5D_i (i = 0, 1, 2) levels after non-radiation phonon interaction from the Eu^{3+}–O^{2-} CT.

4. Conclusions

Pure and Eu^{3+} doped Sr_2CeO_4 were prepared by the polymer-network gel method. The structure and luminescence of Sr_2CeO_4:Eu^{3+} phosphors were investigated. A broad emission band originating from Sr_2CeO_4 host and Eu^{3+} emission lines in the blue, green, and red regions coexisted. The emissions from the higher excited state ^5D_i (i = 1, 2) apart from $^5D_0$ of Eu^{3+} ions were observed. Besides, the red emission $^5D_0$–$^7F_2$ intensity increased as the Eu^{3+} ion concentration increased from 1 to 5 mol%. These unusual luminescent properties are due to the low vibration energy of Sr_2CeO_4 host-lattice and different energy transfer process from host to activator. Furthermore, the high efficiency of the energy transfer suggested that the Sr_2CeO_4 crystal structure could form the base for the creation of luminescence materials that are effective in different spectral ranges.

Acknowledgements

This work was financially supported by Education Ministry Innovation Research Team project (IRT 0972), National Natural Science Foundation of China (Grant No. 60976018) and Natural Science Foundation of Shanxi Province (Grant No. 2007011066).

References

[1] J.L. Huang, L.Y. Zhou, Z.L. Wang, Y.W. Lan, Z.F. Tong, F.Z. Gong, J.H. Sun, L.P. Li, J. Alloys Compd. 487 (2009) L5.
[2] G.F. Wang, Q.Y. Mu, T. Chen, Y.D. Wang, J. Alloys Compd. 493 (2010) 202.
[3] N. Perea, G.A. Hirata, Thin Solid Films 497 (2006) 177.
[4] S.V. Mahajan, J.H. Dickerson, J. Alloys Compd. 488 (2009) 574.
[5] E. Danielson, M. Devenney, D.M. Giaquinta, J.H. Golden, R.C. Haushalter, E.W. McFarland, D.M. Poojary, C.M. Reaves, W.H. Weinberg, X.D. Wu, Science 279 (1998) 837.
[6] O.A. Serra, V.P. Severino, P.S. Calefi, S.A. Cicillini, J. Alloys Compd. 323/324 (2001) 667.
[7] X.M. Liu, Y. Luo, J. Lin, J. Cryst. Growth 290 (2006) 266.
[8] T. Hirai, Y. Kawamura, J. Phys. Chem. B 109 (2005) 5569.
[9] C.X. Zhang, W.J. Jiang, X.J. Yang, Q.F. Han, Q.L. Hao, X. Wang, J. Alloys Compd. 474 (2009) 287.
[10] C.H. Lu, T.Y. Wu, C.H. Hsu, J. Lumin. 130 (2010) 737.
[11] R. Ghildiyal, P. Page, K.V.R. Murthy, J. Lumin. 124 (2007) 217.
[12] I.M. Nagpure, K.N. Shinde, V. Kumar, O.M. Ntwaeaborwa, S.J. Dhoble, H.C. Swart, J. Alloys Compd. 492 (2010) 384.
[13] C.H. Lu, C.H. Huang, B.M. Cheng, J. Alloys Compd. 473 (2009) 376.
[14] T. Nishida, T. Ban, N. Kobayashi, Appl. Phys. Lett. 82 (2003) 3817.
[15] C.H. Hsu, C.L. Liaw, C.H. Lu, J. Alloys Compd. 489 (2010) 445.
[16] L. Li, S.H. Zhou, S.Y. Zhang, Chem. Phys. Lett. 453 (2008) 283.
[17] N. Perea-Lopez, J.A. Gonzalez-Ortega, G.A. Hirata, Opt. Mater. 29 (2006) 43.
[18] X.H. He, J. Rare Earth 25(s) (2007) 50.
[19] X.H. He, W.H. Li, Q.F. Zhou, Mater. Sci. Eng. B 134 (2006) 59.
[20] X.Z. Xiao, B. Yan, J. Phys. Chem. Solids 69 (2008) 1665.

[21] A. Nag, T.R. Narayanan Kutty, J. Mater. Chem. 13 (2003) 370.
[22] T. Hirai, Y. Kawamura, J. Phys. Chem. B 108 (2004) 12763.
[23] O. Viagin, A. Masalov, I. Ganina, Y. Malyukin, Opt. Mater. 31 (2009) 1808.
[24] T. Xian, H. Yang, X. Shen, J.L. Jiang, Z.Q. Wei, W.J. Feng, J. Alloys Compd. 480 (2009) 889.
[25] X.A. Chen, C.Y. Yang, X.N. Chang, H.G. Zang, W.Q. Xiao, J. Alloys Compd. 492 (2010) 543.
[26] Y.H. Wang, Z.Y. Zhang, J.C. Zhang, Y.H. Lu, J. Solid State Chem. 182 (2009) 813.
[27] M. Othman, E. Kasap, N. Korozlu, J. Alloys Compd. 496 (2010) 226.